
Article:
Ritterskamp, D., Bearup, D. orcid.org/0000-0001-8524-7659 and Blasius, B. (2016) A new dimension: Evolutionary food web dynamics in two dimensional trait space. Journal of Theoretical Biology, 405. pp. 66-81. ISSN 0022-5193

https://doi.org/10.1016/j.jtbi.2016.03.042

A New Dimension: Evolutionary Food Web Dynamics in two Dimensional Trait Space

Daniel Ritterskamp*, Daniel Bearup, Bernd Blasius

CvO University Oldenburg, ICBM, Carl-von-Ossietzky-Strasse 9-11, 26111 Oldenburg, Germany

Abstract

Species within a habitat are not uniformly distributed. However this aspect of community structure, which is fundamental to many conservation activities, is neglected in the majority of models of food web assembly. To address this issue, we introduce a model which incorporates a second dimension, which can be interpreted as space, into the trait space used in evolutionary food web models. Our results show that the additional trait axis allows the emergence of communities with a much greater range of network structures, similar to the diversity observed in real ecological communities. Moreover, the network properties of the food webs obtained are in good agreement with those of empirical food webs. Community emergence follows a consistent pattern with spread along the second trait axis occurring before the assembly of higher trophic levels. Communities can reach either a static final structure, or constantly evolve. We observe that the relative importance of competition and predation is a key determinant of the network structure and the evolutionary dynamics. The latter are driven by the interaction – competition and predation – between small groups of species. The model remains sufficiently simple that we are able to identify the factors, and mechanisms, which determine the final community state.

Keywords: Spatial food webs, Higher dimensional trait space, Network structure, Evolutionary dynamics, Large community-evolution models

*Corresponding author

Email addresses: daniel.ritterskamp@outlook.de (Daniel Ritterskamp), daniel.bearup@uni-oldenburg.de (Daniel Bearup), blasius@icbm.de (Bernd Blasius)

1. Introduction

Ecologists have long been interested in the complex structures exhibited by empirical food webs, the first studies dating back at least to the seventeenth century (see [24, 23]). Food webs describe the structure of 'who-eats-whom' in a community and constitute one of the most fundamental levels of biological organization. This structural richness has inspired theoretical approaches to capture food web topology and dynamics in terms of mathematical models. Most theoretical food web studies can be separated into two categories: generating food web structures or describing population dynamics.

On the one hand, narrative statistical models have been put forward that combine stochastic elements with simple link assignment rules and allow networks of trophic interactions between species that closely resemble empirical food webs to be synthesised [23]. The most prominent examples are the cascade model [19], the niche model [70] and the random model [34]. Models of this type are able to provide a detailed understanding of the structural complexity of food webs [60, 72, 61] and, with certain refinements, produce ecologically reasonable food web structures [54, 3, 52]. However, the population dynamics of the resultant community are not addressed within this framework and must be modelled separately.

Thus, a separate stream of research has focused on dynamical models, describing the temporal change of populations within a food web structure. These models have proven to be able to capture a huge range of dynamic complexities, such as population cycles, multi-stability and chaotic dynamics. However, they contain a large number of free parameters that have to be carefully chosen to fit to empirical food webs, without over fitting the model [29, 68]. This problem is elegantly solved in allometric food web models, which were introduced by Yodzis and Innes [74] and extensively studied since [14, 9]. These models automatically determine the model parametrization using allometric scaling to determine how species dynamics vary with bodysize. Where the food web structure can be determined a priori such models can accurately predict the dynamics of ecological communities [10, 28]. However, just as statistical models cannot describe population dynamics, dynamical models cannot be used to generate food web structure, since the food web topology is required to initialize the model.

These two approaches are combined in population based, evolutionary food web models [16, 22, 67, 56, 65, 66]. One prominent class of such models

are niche based evolutionary food web models, which were introduced by Loeuille and Loreau [40]. In these models each species is characterised by a position, related to its bodysize, on a continuous niche axis. The strengths of interactions between species are then simply determined by their pairwise distances along the niche axis and allometric scaling with bodysize. New species can be added to the community simply by assigning them a trait value, with the change in food web topology being determined automatically. As such they provide a simple means to capture the combinatorial increase in possible food web structures that occurs as community size increases.

Niche based coevolutionary food web models were examined in great detail. Refinements of the original model [40] studied, for example: the influence of trade-offs in resource consumption on the network structure [37]; the emergence of diversification by incorporating gradual evolution [11]; and evolvable shapes of the feeding interaction kernels to produce more realistic food webs [5]. However these studies also revealed that niche based evolutionary models do not generate the degree of variety in food web structure [4] that is observed in empirical food webs. Additionally, whereas such models typically generate a single dynamic regime [40, 11, 5], it is assumed that empirical food webs display a range of dynamical states [73, 50].

This limited variety could be related to the fact that these niche based evolutionary models consider only a single evolutionary trait – bodysize. Several studies have raised the question whether a larger number of traits may be necessary to realistically describe species interactions or food web intervality [3, 47, 62, 25]. In this case, trophic niche space would be spanned by other factors or phenotypic traits, apart from bodysize. Subsequent studies showed that the dimensionality of trophic niche space has strong implications for food web structure and the adequate dimensionality of trophic niche space remains an ongoing debate in the food web literature [18, 52, 55, 2, 44].

Thus, a higher dimensional trait space could resolve the aforementioned limitations in the structural and dynamical variety of niche based evolutionary food web models. Zhang et al. [75] constructed one example of such a model by incorporating a spatial dimension into the evolutionary food web framework. In this model each species is characterized by two traits: bodysize and a spatial habitat preference, used to characterize a population's distribution in space. The strength of feeding interactions was modelled as a function of the pairwise distance between predator and prey species in the two-dimensional niche space. The analysis by Zhang et al. [75] showed that the second trait dimension had significant influence on the emerging size

spectra and maximal trophic levels. However, this study did not investigate how the interaction parameters in the two dimensional niche space influence the variety of food web structures and dynamics which can emerge.

In this study, we propose a conceptual evolutionary food web model that describes the population dynamics of a community of species in a two-dimensional niche space, characterized by bodysize and a second abstract trait. Our model is similar to that of Zhang et al. [75] although we follow closely Loeuille and Loreau [40] when determining interactions along the bodysize axis and introduce new species via an evolutionary algorithm. Most notably, we model competitive interaction between species along the second trait dimension. Thus, our model unifies the seminal MacArthur-Levin's model of competition on a niche axis with an evolutionary food web model on a bodysize axis. In our model, species are described by their trait values in a two dimensional space and their interactions – feeding and competition – by the niche overlap in this space. The second trait can be interpreted in a variety of ways, for example as a vertical position in a water column, day time of activity, habitat preference, phylogeny, a hidden gradient (e.g. temperature, salinity, rainfall, day length) or it may simply be regarded as a spatial coordinate.

Our primary goal in this study is to investigate the diversity of food web structure and dynamics that emerges when such a second trait axis is introduced to the evolutionary food web framework. Note that using a conceptual model that remains sufficiently simple, within the evolutionary food web framework, it is possible to obtain insights into the factors and mechanisms underlying particular phenomena. Thus a secondary aim of this study will be to identify possible ecological processes that are responsible for greater food web diversity. Using intensive numerical simulations we show that the additional trait axis allows the emergence of communities with a much greater range of network structures, similar to the diversity observed in real ecological communities. Thereby, the combined interplay of evolutionary and population dynamics gives rise to a plethora of community structures and dynamical outcomes, such as evolutionary outbursts where a top-layer of morphs at high bodysize spontaneous emerges and collapses, or directed evolutionary motion, where species are co-evolutionarily driven towards smaller bodysizes. Community emergence follows a consistent pattern with spread along the second trait axis occurring before the assembly of higher trophic levels. Communities can reach either a static final structure, or constantly evolve. We observe that the relative importance of competition and predation

is a key determinant of the network structure and the evolutionary dynamics. Finally, we will show that the model produces ecologically reasonable results by undertaking a limited comparison to empirical food webs.

2. Model

We develop an evolutionary food web model, describing the dynamics of one resource and a variable number of evolving morphs ($i = 1, ...N$). We use the term morph instead of species, since we neglect reproductive isolation and the underlying isolation mechanism that leads to speciation. Each morph is characterised by two evolutionary traits, logarithmic bodysize z_i, and an abstract trait x_i, as well as a population biomass density B_i, which varies due to interactions with other morphs. Following MacArthur and Levins [42], the strength of morph interactions is determined by their pairwise distance in the two dimensional trait space: competitive interactions decrease with the distance between two morphs in either dimension; and so do feeding interactions with regard to their abstract traits, but they are maximized for a certain offset in the bodysize direction. This follows from empirical observations that species typically consume prey that is a certain fraction smaller than themselves [69, 12]. The resource of concentration R has a bodysize $z_R = 0$ and is continuously distributed along the abstract trait axis. The trait axis has a length of L, however we use periodic boundaries to simulate an infinite range [59].

The model itself can be divided into two processes, the population dynamics of the community and an evolutionary algorithm, which occur on separated time scales. The population dynamics determine the variation in each morph's biomass B_i. The evolutionary algorithm operates on a slower time scale, introducing new morphs after the population dynamics have approached a steady state. We now consider each component in more detail.

2.1. Population Dynamics

The change of biomass B_i of morph i is given by Lotka-Volterra equations, accounting for reproduction by consuming other morphs and the resource,

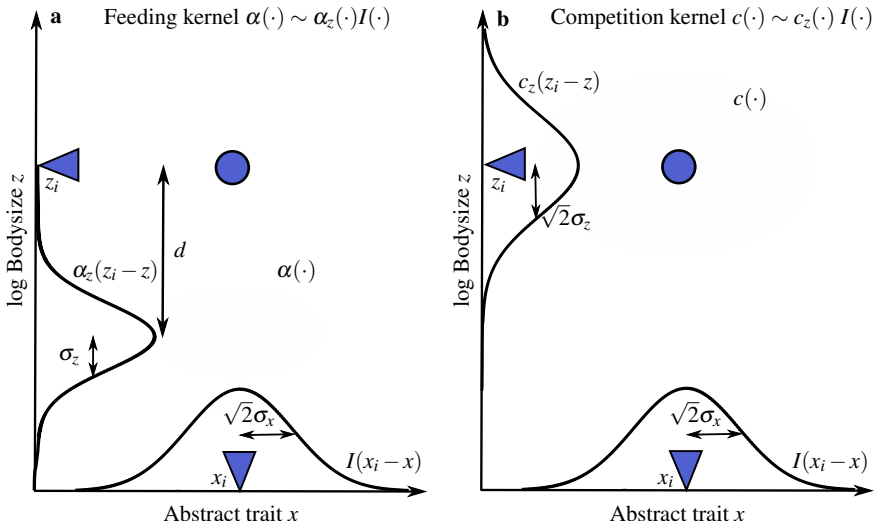

Figure 1: Interaction kernels of the two dimensional food web model. The plots show the interaction strength described by two-dimensional Gaussian functions (ellipses) of a species with trait value x_i and bodysize z_i (indicated by blue circle and triangles). **a:** The feeding kernel $\alpha(\cdot)$ is modelled as the product of the bodysize feeding kernel $\alpha_z(z_i - z)$, with a maximum at $z = z_i - log(d)$ and a width of σ_z, and the dependency on the abstract trait $I(x_i - x)$, centred around $x = x_i$ with a width of $\sqrt{2}\sigma_x$. **b:** The competition kernel $c(\cdot)$ is modelled as the product of $I(x_i - x)$ and the competition kernel in bodysize $c_z(z_i - z)$ with a width of $\sqrt{2}\sigma_z$, given by the overlap of the bodysize feeding kernels of the competing morphs. Since the competition kernel is determined by niche overlap the competition ranges are not independent parameters (see Fig. A.8).

and losses due to mortality and respiration, predation and competition

$$\frac{dB_i}{dt} = B_i \Big(\underbrace{f_0\; a(z_i) \sum_{j=1, i\neq j}^{N} \alpha(z_i, z_j, x_i, x_j) B_j + f_0\; a(z_i) \int_0^L dx\; \alpha(z_i, z_R, x_i, x)R(x)}_{Reproduction} - \underbrace{m_0\; a(z_i)}_{Mortality} - \underbrace{\sum_{j=1, i\neq j}^{N} a(z_j)\alpha(z_j, z_i, x_j, x_i) B_j}_{Predation\ loss} - \underbrace{\sum_{j=1}^{N} c(z_i, z_j, x_i, x_j) B_j}_{Competition} \Big), \tag{1}$$

where f_0 is the conversion efficiency and m_0 is the basic mortality rate. Feeding interactions and biomass loss rates scale according to allometric relations with bodysize [48], which is expressed by $a(z_i) = 10^{-0.25 z_i}$.

The feeding kernel $\alpha(\cdot)$ describes the ability of predator i to consume prey j. We assume that it is the product of two functions (Fig. 1a), describing the bodysize and abstract trait dependency,

$$\alpha(z_i, z_j, x_i, x_j) = \alpha_0 \; \alpha_z(z_i, z_j) \; I(x_i, x_j), \tag{2}$$

with α_0 being the attack strength.

Empirical studies suggest that feeding interactions depend on the logarithmic bodysize distances between morphs and are hump shaped [69, 12]. To represent this, we express the bodysize dependency of the feeding kernel by a Gaussian function,

$$\alpha_z(z_i, z_j) = \frac{1}{\sigma_z \sqrt{2\pi}} \exp\Big(- \frac{(z_i - z_j - \log(d))^2}{2\sigma_z^2} \Big), \tag{3}$$

where d is the optimal predator-prey bodysize distance and σ_z corresponds to the feeding range of a morph.

Even though cannibalism is not uncommon in some cases [27], we explicitly exclude cannibalistic feeding interactions ($\alpha(z_i, z_i, x_i, x_i) = 0$). The alternative, in this model, is to require that every morph be a cannibal which also seems unrealistic. Nonetheless, we expect our results to be relatively general, since cannibalism can be described by an additional contribution to the intra-specific competition strength; this would slightly decrease the biomass of the cannibalistic morph [5], but the general evolutionary outcome would not be affected. This is confirmed by numerical investigations which showed that that the qualitative model outcomes are independent of this choice.

The dependency of the feeding kernel on the abstract trait is given by

$$I(x_i, x_j) = \frac{1}{\sigma_x \sqrt{4\pi}} \exp\Big(- \frac{(|x_i - x_j|)^2}{4\sigma_x^2} \Big), \tag{4}$$

which is of Gaussian shape with a width of $\sqrt{2}\sigma_x$ and states the interaction strength of two morphs along the abstract trait axis, see Fig A.8 for its derivation.

Motivated by the model of MacArthur and Levins [42], the competition

kernel $c(\cdot)$ is determined by the niche overlap between two morphs in the two dimensional trait space (Fig 1b), as the overlap in abstract space $I(\cdot)$ and the prey they have in common $c_z(\cdot)$,

$$c(z_i, z_j, x_i, x_j) = c_0 \; c_z(z_i - z_j) \; I(x_i, x_j), \tag{5}$$

where c_0 is the competition strength and

$$c_z(z_i - z_j) = \frac{1}{\sigma_z 2\sqrt{\pi}} \exp\Big(- \frac{(z_i - z_j)^2}{4\sigma_z^2} \Big). \tag{6}$$

The latter is calculated by the overlap of the bodysize feeding kernels $\alpha_z(\cdot)$ of both morphs, see Fig. A.8 for more details. The width of the feeding and competition kernels in both dimensions are determined by the same parameters, with competition range being by a factor of $\sqrt{2}$ larger than the feeding range.

Unlike the evolving morphs, the resource has a constant bodysize and is continuously distributed along the abstract trait axis. The dynamics of the resource are given by the following chemostat equation

$$\frac{dR(x)}{dt} = I - eR(x) - \sum_{j=1}^{N} \alpha(z_j, z_R, x_j, x) B_j \; R(x). \tag{7}$$

Here, the first and second terms represent a constant input and an outflow relative to the resource biomass and the final term describes losses due to consumption by the morphs in the system.

Following the original formulation of these models by MacArthur and Levins [42] and Loeuille and Loreau [40], we intentionally keep our model as simple as possible. In particular, we describe predation rates using linear, rather than more realistic [35] functional responses. This allows us to truly unify both models. If all species have the same bodysize, our model reduces to the MacArthur and Levins model of competition along a niche axis [42]. In contrast, if all species have the same value of their abstract trait our model reduces to an evolutionary food web model, similar to Loeuille and Loreau [40].

2.2. Evolutionary Dynamics

Every t_m time units a randomly chosen morph k mutates, and a mutant m is added to the system, with a new abstract trait $x_m \in [x_k - \Delta_x, x_k + \Delta_x]$, and logarithmic bodysize $z_m \in [z_k - \Delta_z, z_k + \Delta_z]$. In our model, the mutant is then introduced with an initial biomass of θ, which is also the extinction threshold. If the biomass B_k of any morph falls below this threshold, as a result of the population dynamics, it is considered to be extinct and is removed from the system.

2.3. Initialization and Parameter Values

Simulations are performed using the Sundials CVODE solver [20] in C++ with absolute and relative errors per time step set to 10^{-12}. The abstract trait axis is discretised by one hundred grid points per unit length and periodic boundaries are applied. All simulations are initialized with the resource (logarithmic bodysize $z_R = 0$ and a concentration of $R(x) = I/e$) and a single evolving morph with an abstract trait of $x_1 = \frac{L}{2}$ and logarithmic bodysize $z_1 = \log(d)$.

The parameters regarding the population dynamics were set to $f_0 = 0.3$, $m_0 = 0.1$, and $log(d) = 2$, following [40]. For the evolutionary parameters we set $\theta = 10^{-10}$ ([4]) and $\Delta_z = \log(2)$, as in [5]. The mutation time t_m is set to 10^5, which is sufficiently high for the population dynamics to reach an equilibrium before the next mutation event. Parameters describing interactions along the abstract trait dimension were fixed as follows: $I = 1000$, $e = 0.1$, $\sigma_x = 0.05$, and $L = 1$. Tests of alternative values of these parameters found that they had no qualitative effect on our results (see Results). As discussed in Section 3 these parameters mainly influence the effective length of the abstract trait axis. Furthermore, we choose a relatively narrow mutation range in this direction, $\Delta_x = 0.08$, to ensure that mutants are similar to their parents. Finally, to reduce the number of free parameters, we set the attack strength, $\alpha_0 = 1.0$, and in the simulations presented in this work we vary the competition strength c_0 and feeding range σ_z as our main control parameters.

2.4. Data Evaluation

Since the evolutionary outcome depends on the sequence of random numbers, we perform one hundred simulation runs for each parameter set, with different seeds. Each simulation runs for 10^{10} time units, if not stated otherwise. To calculate the network characteristics we collect 20 networks from

each simulation run, each $5 \cdot 10^8$ time units, starting at a time of $5 \cdot 10^8$ to omit the initial assembly phase. This produces a total of 2000 networks for each parameter set. To calculate the network structure we follow [5] and remove all links that supply less than 75% of the biomass contributed by the average link. This cut-off criterion depends on the feeding kernel and the prey's biomass density and therefore mimics sampling limits in empirical data.

The emerging networks are compared to empirical data, in particular the 50 aquatic food webs in the Adirondack lake data set [64] (see Havens [32] for details concerning the construction of these food webs). Since the model can only produce networks with one resource, we treat all species in the first trophic level of the empirical food webs as a single species, as proposed by [54]. The trophic level is calculated using the prey-averaged trophic level, for the empirical data, and the flow-based trophic level, for networks obtained from simulations [71].

3. Results

We now investigate how morph interactions influence the emergence of the network structure and evolutionary behaviour. A systematic screening of the parameter subspace, composed of competition strength c_0 and feeding range σ_z, reveals regions that are dominated by three distinct community types (Fig. 2). (We say that a community type is dominant when 80% of simulated outcomes are of that type.) The first community type is characterised by a complete absence of trophic structure. A single trophic level builds up, consisting of morphs that consume the resource, but no further trophic levels emerge. The areas of parameter space where such communities dominate are denoted Region I. The second type of community has trophic structure and is evolutionarily static. That is, after an initial dynamic phase of community assembly, the morphs, and the interactions between them, become fixed. Such food webs dominate in Region II. The third type of community has trophic structure and is evolutionarily dynamic. The morphs in such communities, and their interactions, change constantly over time and leading to the temporary emergence of higher trophic levels (evolutionary outbursts) and cases where a given morph progressively decreases its body-size (evolutionary downwards movement). Region III is dominated by food webs of this type. In addition, we observe an additional area that is not dominated by a specific behaviour which we refer to as Region IV.

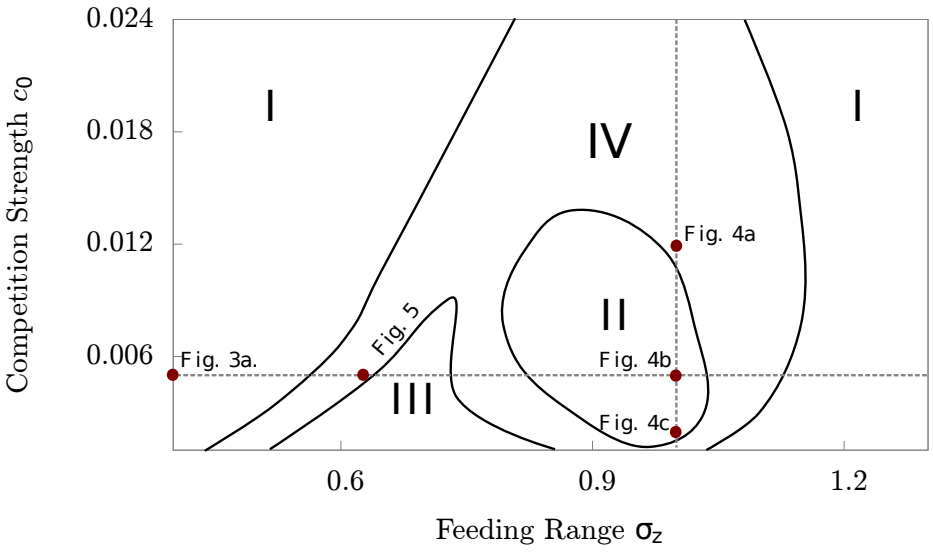

Figure 2: Effect of feeding range σ_z and competition strength c_0 on the model outcome. Four regions in parameter space occur, three of them are dominated by a particular type of community: Region I is dominated by communities with no trophic structure; Region II by evolutionarily static food webs; and Region III by evolutionarily dynamic food webs. In between these, an additional region occurs that is not dominated by a specific community type (i.e., less than 80% of simulated communities correspond to a single state, see also Fig. A.9 for the frequencies of each state), which is referred to as Region IV. Points denote examples further analysed in Figs. 3-5 and dotted lines represent the cross sections shown in Figs. 6 and 7.

These regions are robust with respect to variation of the parameters governing interactions along the abstract trait dimension (see Section 2.3 for a specific list). Increasing the level of resources available, determined by I and e, (beyond the level necessary to support multiple bodysize layers) or the length of the abstract trait axis L, increases the number of morphs that can coexist, but does not change the food web type, whereas a larger value of σ_x is equivalent to a decrease in available resources or an increase in L.

3.1. Communities with no trophic structure (Region I)

Region I is dominated by evolutionarily static communities with a single trophic layer of primary consumers. This region is split into two sub-regions with distinct community characteristics, see Fig. 3. For small feeding ranges σ_z, the community contains many morphs with nearly identical bodysizes packed densely along the abstract trait axis. Consequently, the distribution of biomass along this axis is nearly uniform. In contrast, for large σ_z, there

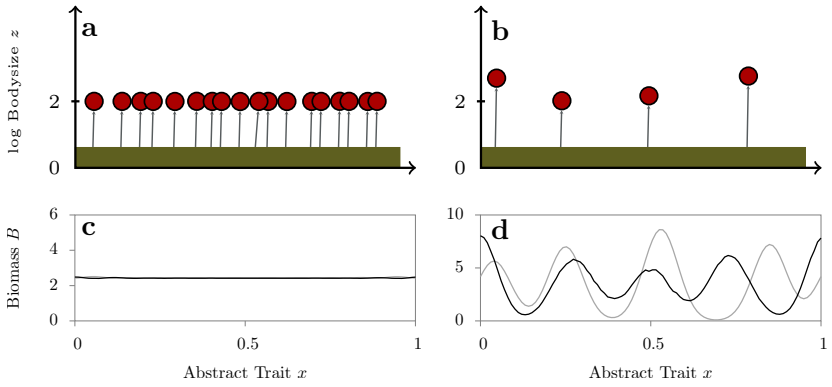

Figure 3: Two characteristic patterns of static communities without trophic structure (Region I), emerging for the case of a narrow feeding range ($\sigma_z = 0.4$, left column) and a large feeding range ($\sigma_z = 1.5$, right column). **a,b:** Positioning of morphs (represented by red circles) in two dimensional trait space. The green bar illustrates the resource. **c,d:** Biomass distribution along the abstract trait axis of the presented network (grey). It is assumed that a morph's biomass is distributed around the abstract trait, x_i, according to a Gaussian of width σ_x (see Fig. A.8). The black line denotes the average over 100 different simulated networks, whereby all biomass distributions are aligned by setting the maximum biomass value to an abstract trait value of zero. Therefore an artificial maximum and a subsequent minimum occur at the edges of the abstract trait axis. **Left column** ($\sigma_z = 0.4$): Dense morph packing along the abstract trait axis of morphs with similar bodysize. The biomass is continuously distributed along the trait axis, with the distributions of the single run and the average overlapping, since the interval between morphs is close to the distribution range along the abstract trait, σ_x. **Right column** ($\sigma_z = 1.5$): Food web wherein morphs keep a maximal characteristic distance to each other in trait space (see averaged distribution). Only four morphs are contained, which differ in bodysize, but are restricted to the same trophic level. In all simulations, the competition strength is fixed to $c_0 = 0.005$.

are relatively few morphs with a much greater diversity in bodysize spaced at relatively broad intervals along the abstract trait axis. In this case, the average biomass distribution displays a regular pattern of biomass peaks (see Section 3.3 for more details)

3.2. Communities with trophic structure

In our simulations, communities with trophic structure emerge with high frequency only for low to intermediate competition strengths c_0 and intermediate feeding ranges σ_z. This was also observed and explained in detail by [41], who studied the emergence of trophic structures in niche based evolutionary food web models by evolutionary branching. However in our model,

after a branching event in bodysize, morphs of similar – though varying – bodysize spread along this abstract trait dimension. Only after the bodysize layer is established across a region of the abstract trait axis, does another branching event become possible, allowing a new layer can emerge. The variation in the bodysizes of morphs along the abstract trait dimension induces variation in the bodysize layer of larger morphs, as these morphs optimise their bodysize to feed on local prey morphs.

As mentioned above, two types of food web emerge, characterised by whether they are static or dynamic on evolutionary time scales. The latter case, evolutionarily dynamic food webs, occurs for small competition strengths and lower feeding ranges. In this parameter range, morphs occupy relatively small niches in the trait space, due to the sharpness of the feeding and competition kernels. Consequently vacant niches are always present, which allows new invasion events to occur frequently. We consider each of these evolutionary behaviours below, beginning with the simpler case of evolutionarily static food webs.

3.2.1. Evolutionarily static food webs (Region II)

Evolutionarily static food webs dominate in Region II (ellipsoid region, Fig. 2). Three representative food webs with different competition strengths c_0 are plotted in Fig. 4. In each case, after an initial assembly phase, the bodysize distribution of the community becomes static (Fig.4a-c). We also observe two patterns in the structure of these communities relative to competition strength.

Firstly, as competition strength decreases the trophic structure of the food webs becomes less regular (Fig. 4d-e). For high c_0 morphs with a similar bodysize tend to have the same trophic level. With decreasing c_0 these trophic level start to merge and for small c_0 a given bodysize range can contain morphs of different trophic levels. Additionally, for high c_0 the food web structure is relatively consistent along the abstract trait axis, while for smaller c_0 values this structure becomes more variable.

This observation is reinforced by the plots of trophic level against log bodysize (Fig. 4j-l). For high c_0 there is a strict hierarchical ordering of morphs by bodysize. As c_0 decreases a concave shoulder emerges, indicating that a morph's role in the food web is less strongly determined by its bodysize. The flat section of these plots, at a trophic level of two, arises from the small number of communities with no trophic structure, which occur in this region (see Section 3.1 and Fig. A.13).

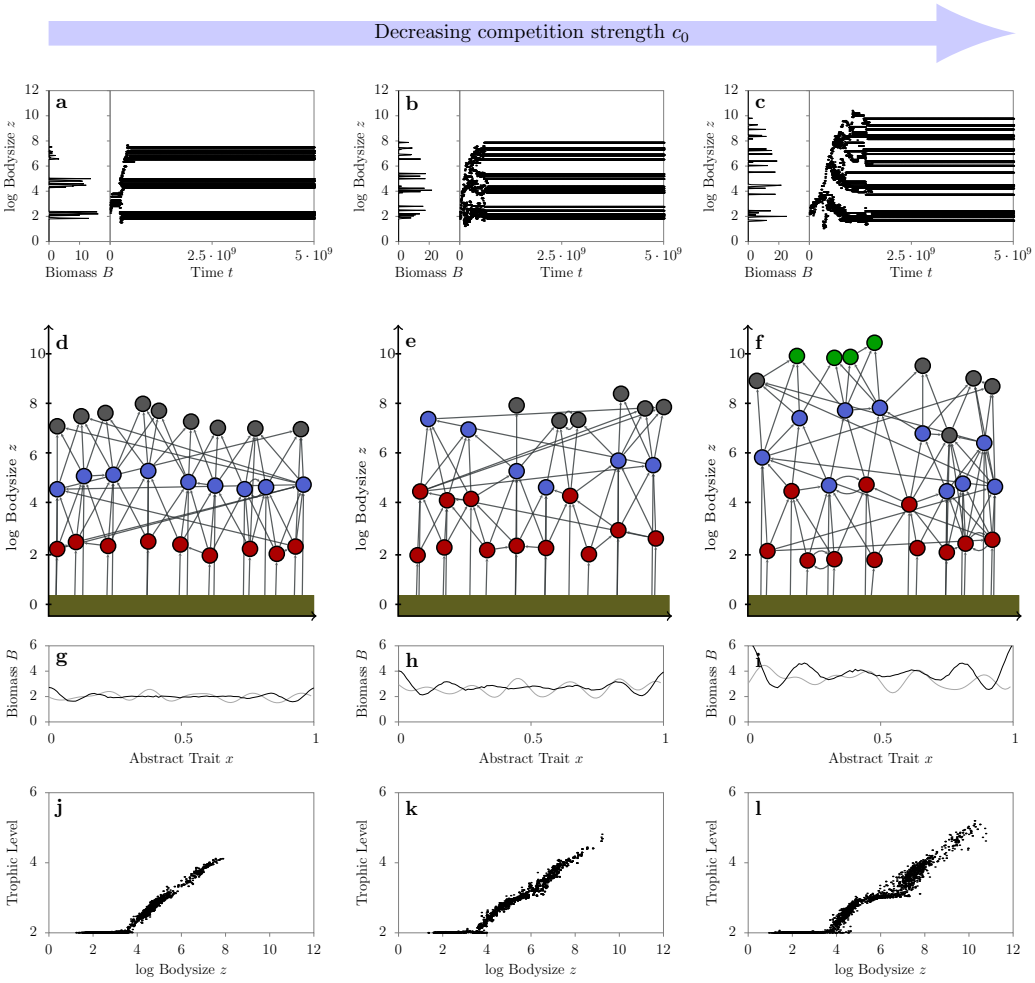

Figure 4: Structure of evolutionarily static food webs (Region II). Each column presents a different competition strength c_0, decreasing from left to right (see Fig. 2 for position in parameter space). **Left column** ($c_0 = 0.012$): Static network with distinct bodysize layers. **Middle column** ($c_0 = 0.005$): Static network with slightly merged bodysize layers. **Right column** ($c_0 = 0.002$): Static network with intertwined bodysize layers. **a,b,c:** Temporal evolution of bodysizes (right panels) and bodysize-biomass histograms (left panels) of specific networks over the last $2.5 \cdot 10^9$ time units. **d,e,f:** Positioning of morphs in two dimensional trait space and interaction network. **g,h,i:** Biomass distribution of all morphs along the abstract axis of the network shown (grey) and the average over 100 aligned biomass distributions (see caption of Fig. 3 for more details). **j,k,l:** Morphs' trophic level against logarithmic bodysize for 100 simulated communities. In all simulations, the feeding range was fixed to $\sigma_z = 1$.

Secondly, structure emerges in the distribution of community biomass along the abstract trait axis as competition strength decreases (Fig. 4g-f). For high c_0 the average biomass distribution along this axis is nearly uniform indicating that fluctuations in biomass occur randomly. As c_0 decreases, regularly spaced peaks emerge in the biomass distribution, suggesting an underlying pattern in the distribution of morphs along this axis. This phenomenon is similar to that observed for communities without trophic structure (Fig. 3c-d), although the differences are less pronounced.

These two patterns, and the underlying mechanism producing them, will be discussed in more detail in Section 3.3.

3.2.2. Evolutionarily dynamic food webs (Region III)

Evolutionarily dynamic food webs dominate in Region III (triangular region, Fig. 2), which is positioned at the lower end of feeding ranges and competition strengths of parameter space for that communities with trophic structure are likely. A characteristic example is shown in Fig. 5. Three distinct bodysize layers are present at all times, but the morph composition changes continuously. Occasionally an additional unstable bodysize layer emerges – the trophic structure of the community changes and the number of morphs temporarily increase – before the bodysize layer collapses again (see Figs. 5a,b,d,e). We refer to this phenomenon as an evolutionary outburst. The waiting times between outbursts and durations of outburst are best described by exponential distributions (Fig. A.10). In addition to evolutionary outbursts, we also observe cases where morphs decrease their bodysize progressively, a phenomenon we refer to as evolutionary downwards movement. This movement can traverse several bodysize layers (Fig. 5c). The biomass distributions for individual networks exhibit small fluctuations, however the average distribution is nearly constant indicating that these fluctuations do not reflect an underlying structure along the abstract trait axis (Fig. 5f).

To gain more insight into the two evolutionary phenomena, outbursts and downward movements, we set up a simple community which can only contain two morphs, a predator and a prey (see Appendix A.1 for details). In this simplified system, the two species co-evolve, with the predator following the prey along abstract trait axis, a phenomenon called red-queen dynamics [1, 53, 21]. In larger systems with several morphs, this process can result in local compaction of morphs with similar bodysizes along the abstract trait axis. Morphs in the same layer generally optimize their pairwise distance along the abstract trait axis to avoid competition. However, if the losses

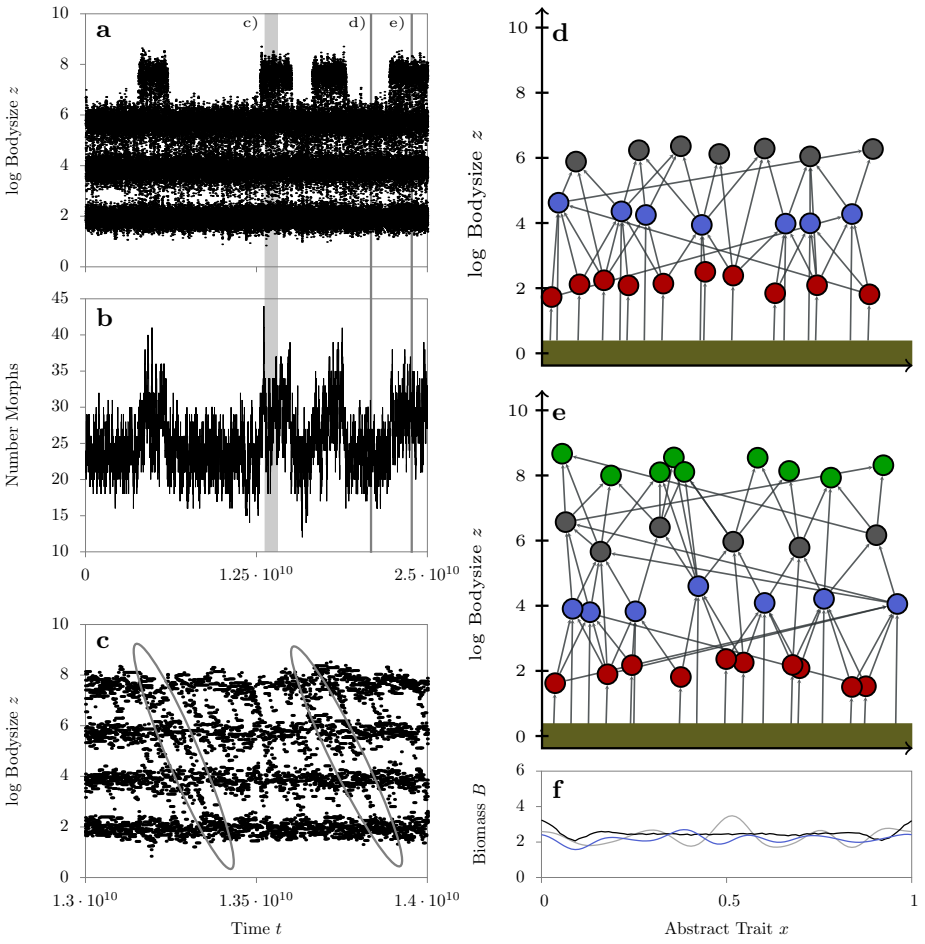

Figure 5: Characteristics of an evolutionarily dynamic food web (Region III). **a:** Temporal behaviour of bodysizes, showing four evolutionary outbursts. **b:** Corresponding total number of morphs as a function of time. **c:** Close up of the temporal development of the bodysizes shown in (**a**), demonstrating the evolutionary downwards movement in bodysize (marked as grey ellipses). The corresponding time window is indicated as grey shaded area in (**a**) and (**b**). **d,e:** Positioning of morphs in trait space and interaction networks, before (**d**) and during (**e**) an evolutionary outburst. Time instances are marked by vertical lines in (**a**) and (**b**). **f:** Biomass distribution along the abstract trait axis of the networks shown in (**d**) (grey) and (**e**) (blue), and averaged over 100 simulation runs (black). Parameter values $c_0 = 0.005$ and $\sigma_z = 0.625$ (see also Fig. 2).

of prey morphs due to predation exceed the losses from increased competition, a coherent evolutionary motion of prey morphs along the abstract trait axis can be induced. As described above, predators will tend to follow this evolutionary movement, causing complex co-evolutionary dynamics [21] and giving rise to transient localised regions of unusually high biomass across all bodysize layers. These regions are able to support larger morphs, producing evolutionary outbursts. This co-evolutionary process also contributes to the termination of outbursts. Over time the top predators repulse their prey morphs, decreasing the biomass density in the bodysize layer immediately below them. As the support for the top predators decreases, they either go extinct or reduce their bodysize by an evolutionary downwards movement. Eventually this happens to all top predators and the evolutionary outburst terminates (see Fig. A.12).

The phenomenon of evolutionary downwards movement can be explained in a similar way. As an alternative to following its prey along the abstract trait axis, a predator can instead evolve downwards in bodysize to feed on lower bodysize layers. When this occurs in a region of lower biomass (due to compaction), the downwards drift may persist over a large number of evolutionary steps and traverse several trophic levels. If no other prey are found, the downward movement will terminate when the morph is able to feed optimally on the resource.

3.3. Community patterns and structural influence of interactions

The competition strength c_0 and feeding range σ_z of morphs determine the type of community that emerges from our model (Fig. 2). In addition we observe that the structural features of particular communities vary with these parameters (Sections 3.1 and 3.2.1). To determine the full extent of these patterns we plot bodysize and average biomass distributions (over 100 realisations for each parameter set) along two cross-sections of the parameter space (Fig. 6). Competition strength varies along Cross-section I, feeding range varies along Cross-section II, in each case the other parameter is held constant.

Figs. 6a & d show how the proportions of community types vary along each cross-section for reference. The average biomass distributions (Figs. 6b & e) show that the patterns previously observed extend across the entire parameter space. In particular as competition strength decreases, or feeding range increases, a regular pattern of biomass peaks emerges along the abstract trait axis. The biomass distribution is almost completely uniform

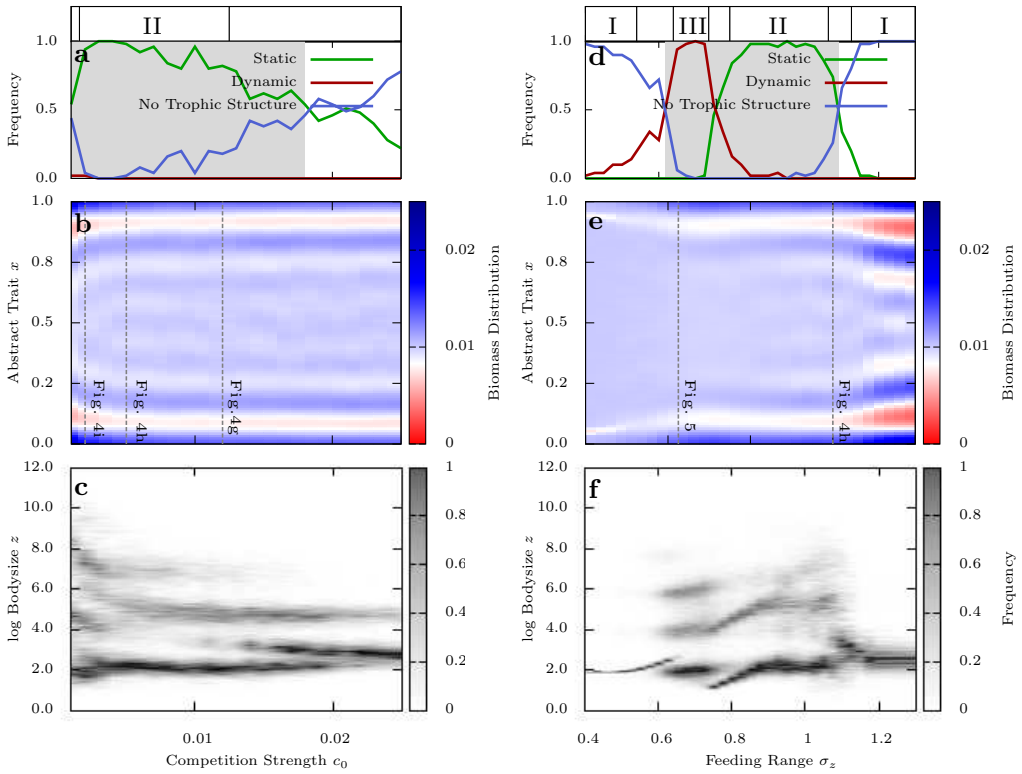

Figure 6: Model outcome along the cross sections through parameter space, shown in Fig. 2. **Left column:** different values of competition strength c_0 for fixed $\sigma_z = 1$ (cross section I). **Right column:** different values of feeding range σ_z for fixed $c_0 = 0.005$ (cross section II). **a,d:** Frequencies of the different community types (indicated by colours) in repeated simulation runs. The grey area marks the regime in which at least 50% of all networks have a trophic structure (i.e., a maximum trophic level greater than 2.5). The bar above this plot indicates the region of parameter space (Roman numeral) in which the parameter combination lies. **b,e:** Average biomass distribution along the abstract trait axis, normalized by the total biomass, as described in Fig. 3. Vertical lines indicate parameter values for which biomass distributions have been shown in Figs. 4-5. **c,f:** Probability density function of log bodysize. The same distributions are shown in Fig. A.13 for the different community structures. For each parameter we averaged over 100 simulation runs.

for small feeding ranges and becomes strongly structured for large feeding ranges. By contrast, the biomass distribution varies relatively little along the competition strength cross-section; a weak structure is present across the majority of the range and strengthens slightly for small c_0. High bodysize diversity, and thus food web complexity, occurs for low c_0 and intermediate σ_z (Figs. 6c & f). Additionally, we observe that bodysize layers become more distinct as c_0 increases, corresponding to more regular food web structure. By contrast, bodysize layers are relatively distinct across the entire feed ranging cross-section, although individual layers do become broader, indicating greater bodysize diversity within layers, as feeding range increases.

These patterns are explained by a trade-off between competition and feeding input. On the one hand, a morph tries to optimise its feeding input by maintaining an optimal logarithmic bodysize separation of $\log(d)$ and a minimal distance in the abstract trait from its prey. On the other hand, it maximizes the distance in trait space to other morphs that feed on the same prey range to minimise competition.

If the competition strength c_0 is high, competition losses exceed the feeding input, and morphs in the same layer increase their separation along the abstract trait. At the same time optimization of the feeding input is important to compensate competition losses. These two constraints combine to create locally optimal niches in trait space, which results in a regular food web structure (e.g. Fig.4d). For lower c_0, these constaints become weaker and consequently the optimal niches are less strictly defined. As a result, the first morph introduced into a niche is often able to fill it, and the network structure becomes irregular (e.g. Fig.4f).

Increasing feeding range σ_z has a similar effect. For small σ_z, predators are highly specialised and thus only a narrow range of mutant bodysizes are viable, resulting in a distinct bodysize network structure. As σ_z increases predators become less specialised and the fitness landscape becomes flatter, allowing greater bodysize diversity and a more irregular network structure. However, this also reduces the feeding input from any given source. Consequently in communities with no trophic structure, where morphs feed only on the resource, even low levels of competition are sufficient to prevent coexistence of morphs in close proximity (e.g. Figs. 3 b & d). This results in a structured biomass distribution, with large biomass maxima separated by a characteristic interval. By contrast, for small feeding ranges, morphs feed efficiently on the resource, and thus the spacing of morphs along the abstract trait axis can be more random (e.g. Figs. 3a & c).

Similar patterns emerge in communities with trophic structure. In food webs with an irregular trophic structure, the morph composition of local regions varies, and consequently so too does the local biomass (e.g. Figs. 4f & i). Regions of high biomass impose a high level of competition on the surrounding area reducing the number of morphs, and hence biomass, that can be sustained, producing a regular biomass pattern. Food webs with more regular trophic structure (e.g. Figs 4d & g) produce a relatively uniform biomass distribution, since the morph composition of any local region is relatively consistent.

3.4. Empirical data: finding model parameters that reproduce natural food webs

In order to show that our model produces ecologically reasonable food webs, and to estimate a ecological parametrisation, we compare the resulting food webs to empirical data, collected from 50 lakes in the Adirondack region [64]. We want to stress that our intention is not provide a comparison between our model and reality (which would require a different model to begin with, including e.g. saturating functional responses). Instead our goal is to find model parameters, which produce a food web with characteristics that are similar to empirical ones.

To compare food web topologies directly, we choose three common community characteristics for comparison: number of morphs, maximal trophic level, and food web connectance. In addition, we consider the fraction of unconsumed potential prey per morph (Fig. 7), which is a measure of intervality, a phenomenon that is not possible if we restrict our model to a one dimensional deterministic trait space (but see [55]). The fraction of unconsumed potential prey per morph is based on the measure for diet contiguity [60, 17] (number of species belonging to gaps in a consumer diet), which is normalised by the total number of species that fall into the bodysize feeding range of a consumer.

Since the model only considers a single resource, following [54], we treated all species of trophic level one in the empirical data as a single species. For each parameter pair along the two cross sections described above (see Section 2.4) we collected 2000 simulated food webs. This ensemble includes communities with a trophic structure (trophic level larger than 2.5, Region II and III) and without (Region I). Therefore changes in the community characteristics could be due to either changes in the ratio of occurrences of these types or due to a transition in the food web structure itself. To separate

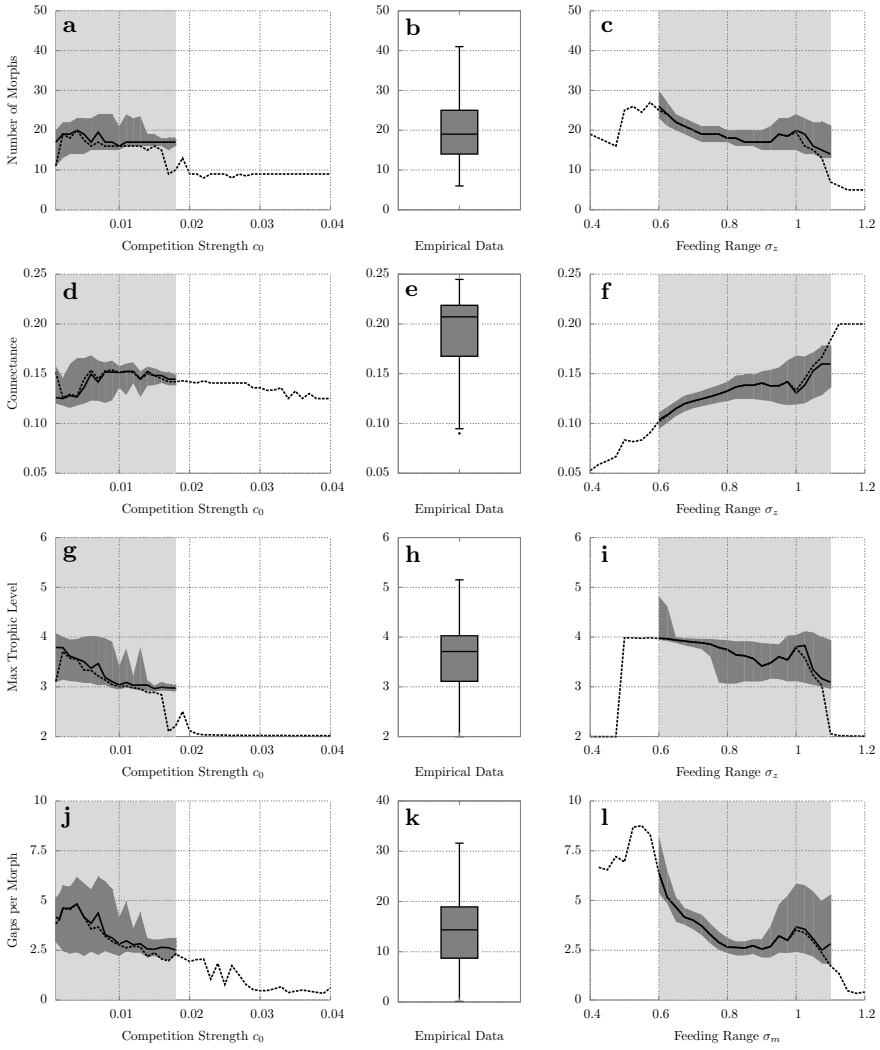

Figure 7: Comparison of characteristics of empirical food webs with simulated networks along the two cross sections. **Left column:** different values of competition strength c_0 for fixed $\sigma_z = 1$ (cross section I). **Middle column:** empirical data, collected from the Adirondack lakes [64] using boxplots (whiskers extend to 1.5 times the interquartile range above and below the upper and lower quartiles.) **Right column:** different values of feeding range σ_z for fixed $c_0 = 0.005$ (cross section II). Along the cross sections the dashed lines represent the median over the complete ensemble of all 100 runs per parameter set. The grey area denotes the parameter regime in which at least 50% of all networks have a trophic structure (trophic level larger than 2.5). Within this area we considered the trophic ensemble, all networks with a trophic structure, and calculated the median (black curve) and the first and third quartile (represented by the dark grey area). **a,b,c:** Total number of morphs, **d,e,f:** connectance, **g,h,i:** maximal trophic level and **j,k,l:** number of unconsumed potential prey per morph. See text for further details.

these effects, we consider a sub-ensemble, consisting only of communities with trophic structure, in the parameter range where at least 50% of all communities have such a structure (light grey area, Fig. 7). The median values of the community characteristics chosen are plotted against the varied parameter values for the complete and trophic ensembles (dashed and solid lines in Fig. 7). The interquartile range for the trophic ensemble is plotted in dark grey and is directly comparable to the interquartile range (grey area) in the empirical values of these characteristics.

The empirical food webs contain a median of 19.1 species, with an interquartile range between 14 and 25. For both cross sections the trophic ensemble is in good agreement with these values, as is the complete ensemble for small feeding ranges (Fig. 7a-c). The median maximal trophic level for the empirical food webs is 3.7 with an interquartile range between 3.1 up to 4.0. The trophic ensembles along each cross section are also in good agreement with these values (Fig. 7g-i).

The median connectance of the empirical food webs is 0.20, with an interquartile range between 0.17 and 0.21. Along the parameter ranges shown here, our simulated communities have lower median connectance (Fig. 7d-f). Only communities with two trophic levels and a small number of morphs (see Fig. 3a) are in good agreement with the empirical values. However by combining the maxima of both cross sections (larger feeding ranges, low competition strength) one can gain networks with a higher connectance.

The median number of unconsumed potential prey per morph of the empirical food webs is 9.9, with an interquartile range between 8.8 and 18.7. In comparison, all simulated food webs underestimate these values and therefore produce lower levels of intervality (Fig. 7j-l). However, higher levels of intervality can be obtained by increasing the length of the abstract trait axis L or decreasing the feeding range σ_z.

Finally, we note that the lower end of extreme values for each characteristic, except the fraction of unconsumed potential prey per morph, (the lower whisker) tends to be in good agreement with the complete ensemble at the upper end of competition strengths and feeding ranges. Empirical food webs with these features typically come from lakes which are relatively poor habitats which, as such, are unable to support a large number of species and high trophic levels. This situation would be most naturally represented by taking a lower value of the resource input I. However the resource limitation could also be expressed by high competition or a low feeding input (which results from relatively unspecialised feeding interactions), so this similarity

is reasonable.

4. Discussion

We have proposed a framework for evolutionary food webs that extends previous models [40, 11, 5, 31] by considering a second niche-space dimension. A similar model was introduced by Zhang et al. [75], but it differs from our model in two notable properties:

First, in contrast to our study Zhang et al., did not incorporate direct competition, but only indirect competition via a shared prey. Thus, our model constitutes a true synthesis of the MacArthur-Levins model of competition on a niche axis with an evolutionary food web model on a bodysize axis. Second, in [75] invaders are drawn from an external (predefined or continuous) species pool, whereas we consider an evolutionary algorithm and therefore reduce the range of invading morphs in dependency of their ancestor trait values. Thus, our species assembly algorithm considers the evolutionary history of a species. When [75] draw invaders from the complete trait space, they observe an ongoing evolutionary change of the food web. In contrast, our extended model produces both types of behaviour, dependent on the characteristics of morph interactions. Furthermore, even for food webs of a given evolutionary type, change in these interactions affects the structural properties of the emergent food webs (e.g. the degree of hierarchy, or distribution along the second niche axis), a phenomenon which has not been seen in many evolutionary food web models.

Our model framework allows us to describe a great variety of communities. This is important, because ecological food webs also display a significant degree of structural, and to a lesser degree dynamical, variety. Freshwater ecosystems have very distinct, hierarchical structures [63, 46], while soil and marine ecosystems are often more amorphous [49]. In addition, a variety of relationships between bodysize and trophic-level – or even the lack of a significant correlation – is reported in empirical studies [51, 38]. While most empirical studies consider food webs to be constant over time, taxon cycles have been observed in small trophic communities [57]. Thus, it is assumed that larger communities can also be dynamic [50].

Since all of these behaviours are reproducible within our relatively simple model, it is possible to identify the model properties, and mechanisms, responsible for these differences. For example, our finding that the relative importance of predation and competition is a key determinant of food

web regularity is supported by empirical observations [36, 33]. Our model suggests that, in highly competitive environments, the pressure to achieve optimal feeding relationships forces the formation of a very rigid food web structure. In contrast, when competition is weaker, the food web structure is looser as the niches within the community are less strictly defined. The degree of specialisation on a given prey type has a similar effect, for the same reasons; we are not aware of a study which has previously made this connection.

The primary technical difference between our model and its predecessors is the extension of the trait space into a second dimension. As such it follows that this second dimension is responsible for the increase in community diversity that we observe. We explain this as follows. In a one dimensional trait space, for instance in the model of Loeuille and Loreau [40], morphs feed on all morphs in the lower trophic level [4] and consequently the whole community is linked, directly or indirectly, by feeding interactions. In a two dimensional trait space this is no longer the case; if morphs are sufficiently far apart in the second dimension, then they have only negligible influence on each other. This allows the emergence of local variation in the food web structure. Additionally the expanded trait space provides morphs with a second evolutionary strategy; in addition to maximising feeding input they can now attempt to avoid predation (or equivalently search for higher densities of prey).

Previous work using evolutionary food web models has focused on the effects of trophic interactions on community structure. However, recent empirical studies have highlighted the influence of spatial factors on the structure of ecological communities [6, 13, 23]. While we have not explicitly included space in our model, it would not be uncommon that the position on the abstract trait axis is associated to a spatial coordinate. This might describe situations where the trait value corresponds to habitat choice or preference for certain environmental characteristics, such as temperature, humidity, or altitude. In such cases, the abstract trait axis can be naturally interpreted as a spatial dimension (e.g. geographic latitude), with the abstract trait value corresponding to the spatial centre of a morph, around which the latter is distributed with a width of σ_x. Consequently, the effects attributed to the second trait dimension, localisation and avoidance, obtain a straightforward spatial interpretation.

On this basis, we can draw two conclusions about the dynamics of spatial community emergence, in particular considering large spatial scales. Firstly,

the spatial assembly (horizontal) of food webs is faster than the trophic (vertical). This occurs because a persistent predator can only emerge after a contiguous region of space has been occupied by their potential prey. Prey in the centre of this region can not avoid the predator evolutionarily, since it is confined by competition with other prey populations. For an unconfined prey, an arms race emerges between predator and prey (Fig. A.11) and the predator eventually focuses on the resource. Secondly, for evolutionary static food webs, propagation of similar morphs across space follows the principle of "First come, first served" [43, 15]. That is, the first viable morph introduced in a spatial region establishes and determines the local food web. This is supported by the observation that the lowest bodysize layer of our simulated food webs is irregular, even when morph feeding is specialised (low feeding range). Thus, the theoretically optimal morph, with bodysize d, does not become established universally. This is a potential explanation for spatial species turnover, that is the empirical observation that the species filling a given ecological niche vary across a landscape [30].

While the dynamics of community emergence are consistent for all food webs generated by our model, the structure of these communities is more variable. As noted above the food web structure is determined by the characteristics of morph interactions. However, we also observe variation in the distribution of biomass across the habitat which appears to be related to variations in the trophic structure of the food web. In particular regular trophic structure induces a uniform biomass distribution, while irregular trophic structure results in regular biomass peaks, see Section 3.3. Spatial variation in food web structure and biomass distribution in homogeneous space have been observed in empirical studies [8, 26, 58, 39], but the two phenomena have not previously been connected.

The dynamics of large communities are difficult to observe experimentally due to the time scales and sampling effort involved [45]. Consequently studies of such phenomena are largely theoretical. However, our results suggest that such dynamics arise from the cumulative effect of interactions between small groups of species which can be more easily studied. In particular, the primary driver of community dynamics in our model, is the coevolution of predator and prey, red-queen dynamics [1, 53, 21]. In small communities this produces characteristic spatio-temporal patterns: bodysize oscillations and spatial chasing (Fig. A.11) which are also observed in experimental studies [36]. In large communities these patterns combine to produce evolutionary outbursts, that is the recurring emergence of higher trophic levels for a limited

period. These are similar to the cycling between high and low trophic community states, discovered by [65, 66]. The build-up of these higher trophic states is due to a prey abundant community, which is similar to our observation. However, in our model, they are not terminated by evolutionary suicide. Instead when the outburst collapses, top predators reduce their bodysize until they are able to sustain themselves in an environment with lower prey density.

The presence of evolutionary outbursts in a community indicates that energy flows from the resource to the higher trophic levels are unstable. Note that the resources supplied are constant, the instability lies in the community structure itself. This is supported by the theoretical study of Zhang et al. [75], which states that the maximal trophic level is constrained by energetic and structural constraints. In our case, the temporary collapse of a population of top predators is not necessarily an indication that a given community is endangered. Nonetheless, we note that changes in resource availability or in species interactions, say due to the introduction of an invasive species, can have similar effects.

One obvious criticism of the spatial interpretation of the second trait axis, is that species dispersal typically occurs on a different time scale to evolutionary adaptation. However, resolving these processes on separate time scales had little effect on the results obtained. Other criticisms include the simplifying assumptions, such as the use of linear functional responses instead of a more realistic multi-species functional response [35], or the fact that competition leads to biomass losses instead of being described as a time consuming factor in the functional response [7]. As explained in the Model section, one major motivation for these simplifications was to preserve the elegance of the model. By keeping the model close to the original formulation in [42] and [40], our model naturally unifies the two seminal models that describe species interactions, either competitive [42] or trophic [40], from species positions in niche space. Future investigations should consider these factors and explore more realistic extensions, such as saturating functional responses which could destabilise the population dynamics, e.g. "paradox of enrichment". Nevertheless, the food webs generated by this model are in relatively good agreement with empirical data. Again, our intention was not to reproduce the fine-structure or empirical communities in detail, as has been done for example in [10, 28]. Instead we explored the structural and dynamical complexities that arise in this conceptual model. Further, we explicitly excluded cannibalism, even though cannibalism is not uncommon in empirical

food webs [27]. We have performed intensive numerical investigations, which confirm that cannibalism does not change the evolutionary behaviour of the model, since the ensemble of evolutionary behaviours stays unchanged. Cannibalism does appear to have an effect on community type for large feeding ranges σ_z, with communities with no trophic structure dominating only for large competition strengths c_0 while for low competition strengths no community type dominates. In addition, communities with no trophic structure in this range display a more homogeneous biomass distribution along the abstract trait axis than was observed without cannibalism (i.e. the regular pattern of biomass peaks disappears in Fig. 3). This is explained by the fact that cannibalism can allow nearly neutral coexistence of very similar morphs and enables morphs of large population sizes to divide into smaller similar populations. However, assuming all species are cannibalistic seems as unrealistic as excluding cannibalism entirely, and thus incorporating cannibalism realistically in this model is a challenge for future work.

In summary, we have shown that, by adding a second trait dimension, with spatial properties, to the evolutionary food web framework, much more of the variety found in ecological communities can be described. Moreover, the framework remains simple enough to allow the factors determining the type of community obtained to be identified. As such this model represents a step towards a more general theory of ecological community assembly, structure and dynamics.

Acknowledgements

This work was supported by the DFG under contract number Dr300/12-1 and 13-1.

[1] Abrams, P.A., 2000. The evolution of predator-prey interactions: Theory and evidence. Annual Review of Ecology and Systematics 31, 79–105.

[2] Allesina, S., 2011. Predicting trophic relations in ecological networks: a test of the allometric diet breadth model. Journal of Theoretical Biology 279, 161–168.

[3] Allesina, S., Alonso, D., Pascual, M., 2008. A general model for food web structure. Science (New York, N.Y.) 320, 658–61.

[4] Allhoff, K.T., Drossel, B., 2013. When do evolutionary food web models generate complex networks? Journal of Theoretical Biology 334, 122 – 129.

[5] Allhoff, K.T., Ritterskamp, D., Rall, B. C. Drossel, B.G.C., 2015. Evolutionary food web model based on body masses gives realistic networks with permanent species turnover. Scientific Report 5.

[6] Amarasekare, P., 2008. Spatial dynamics of foodwebs. Annual Review of Ecology, Evolution, and Systematics 39, 479–500.

[7] Beddington, J.R., 1975. Mutual interference between parasites or predators and its effect on searching efficiency. Journal of Animal Ecology 44, 331–340.

[8] Berg, M.P., Bengtsson, J., 2007. Temporal and spatial variability in soil food web structure. Oikos 116, 1789–1804.

[9] Binzer, A., Brose, U., Curtsdotter, A., Eklf, A., Rall, B.C., Riede, J.O., de Castro, F., 2011. The susceptibility of species to extinctions in model communities. Basic and Applied Ecology 12, 590 – 599.

[10] Boit, A., Martinez, N., Williams, R., Gadeke, U., 2012. Mechanistic theory and modelling of complex food-web dynamics in lake constance. Ecology Letters 15, 594–602.

[11] Brännström, Å., Loeuille, N., Loreau, M., Dieckmann, U., 2011. Emergence and maintenance of biodiversity in an evolutionary food-web model. Theoretical Ecology 4, 467–478.

[12] Brose, U., Ehnes, R.B., Rall, B.C., Vucic-Pestic, O., Berlow, E.L., Scheu, S., 2008. Foraging theory predicts predatorprey energy fluxes. Journal of Animal Ecology 77, 1072–1078.

[13] Brose, U., Ostling, A., Harrison, K., Martinez, N.D., 2004. Unified spatial scaling of species and their trophic interactions. Nature 428, 167–171.

[14] Brose, U., Williams, R.J., Martinez, N.D., 2006. Allometric scaling enhances stability in complex food webs. Ecology Letters 9, 1228–1236.

[15] Burke, C., Steinberg, P., Rusch, D., Kjelleberg, S., Thomas, T., 2011. Bacterial community assembly based on functional genes rather than species. Proceedings of the National Academy of Sciences 108, 14288–14293.

[16] Caldarelli, G., Higgs, P.G., McKane, A.J., 1998. Modelling coevolution in multispecies communities. Journal of Theoretical Biology 193, 345 – 358.

[17] Capitán, J.A., Arenas, A., Guimerà", R., 2013. Degree of intervality of food webs: From body-size data to models. Journal of Theoretical Biology 334, 35 – 44.

[18] Cohen, J.E., 1977. Food webs and the dimensionality of trophic niche space. Proceedings of the National Academy of Sciences 74, 4533–4536.

[19] Cohen, J.E., Newman, C.M., 1985. A stochastic theory of community food webs: I. models and aggregated data. Proceedings of the Royal Society of London. Series B, Biological Sciences 224, 421–448.

[20] Cohen, S.D., Hindmarsh, A.C., 1996. CVODE, A Stiff/Nonstiff ODE Solver in C. Computers in Physics 10, 138–143.

[21] Dommar, C., Ryabov, A., Blasius, B., 2008. Coevolutionary motion and swarming in a niche space model of ecological species interactions. The European Physical Journal Special Topics 157, 223–238.

[22] Drossel, B., Higgs, P.G., Mckane, A.J., 2001. The influence of predatorprey population dynamics on the long-term evolution of food web structure. Journal of Theoretical Biology 208, 91 – 107.

[23] Dunne, J.A., 2009. Food webs, in: Meyers, R.A. (Ed.), Encyclopedia of Complexity and Systems Science. Springer, pp. 3661–3682.

[24] Egerton, F.N., 2007. Understanding food chains and food webs, 17001970. Bulletin of the Ecological Society of America 88, 50–69.

[25] Eklöf, A., Jacob, U., Kopp, J., Bosch, J., Castro-Urgal, R., Chacoff, N.P., Dalsgaard, B., de Sassi, C., Galetti, M., Guimares, P.R., Lomscolo, S.B., Martn Gonzlez, A.M., Pizo, M.A., Rader, R., Rodrigo, A., Tylianakis, J.M., Vzquez, D.P., Allesina, S., 2013. The dimensionality of ecological networks. Ecology Letters 16, 577–583.

[26] Ettema, C.H., Wardle, D.A., 2002. Spatial soil ecology. Trends in Ecology & Evolution 17, 177 – 183.

[27] Fox, L.R., 1975. Cannibalism in natural populations. Annual review of ecology and systematics 6, 87–106.

[28] Fung, T., Farnsworth, K.D., Reid, D.G., Rossberg, A.G., 2015. Impact of biodiversity loss on production in complex marine food webs mitigated by prey-release. Nat Commun 6.

[29] Fussmann, G.F., Heber, G., 2002. Food web complexity and chaotic population dynamics. Ecology Letters 5, 394–401.

[30] Gaston, K.J., Blackburn, T.M., 1995. Birds, body size and the threat of extinction. Philosophical Transactions of the Royal Society of London B: Biological Sciences 347, 205–212.

[31] Hartvig, M., 2011. Food web ecology: individual life-histories and ecological processes shape complex communities. Ph.D. thesis.

[32] Havens, K., 1992. Scale and structure in natural food webs. Science 257, 1107–1109.

[33] Hebblewhite, M., Merrill, E.H., 2009. Trade-offs between predation risk and forage differ between migrant strategies in a migratory ungulate. Ecology 90, 3445–3454.

[34] Heckmann, L., Drossel, B., Brose, U., Guill, C., 2012. Interactive effects of body-size structure and adaptive foraging on food-web stability. Ecology Letters 15, 243–250.

[35] Holling, C.S., 1959. The components of predation as revealed by a study of small-mammal predation of the european pine sawfly. The Canadian Entomologist 91, 293–320.

[36] Holomuzki, J.R., 1986. Predator avoidance and diel patterns of microhabitat use by larval tiger salamanders. Ecology 67, 737–748.

[37] Ingram, T., Harmon, L.J., Shurin, J.B., 2009. Niche evolution, trophic structure, and species turnover in model food webs. The American Naturalist 174, 56–67.

[38] Jennings, S., Pinnegar, J.K., Polunin, N.V.C., Warr, K.J., 2002. Linking size-based and trophic analyses of benthic community structure. Marine Ecology Progress Series 226, 77–85.

[39] Laverman, A., Borgers, P., Verhoef, H., 2002. Spatial variation in net nitrate production in a n-saturated coniferous forest soil. Forest Ecology and Management 161, 123 – 132.

[40] Loeuille, N., Loreau, M., 2005. Evolutionary emergence of size-structured food webs. Proceedings of the National Academy of Sciences of the United States of America 102, 5761–5766.

[41] Loeuille, N., Loreau, M., 2009. Emergence of complex food web structure in community evolution models, in: Verhoef, H.A., J., M.P. (Eds.), Community Ecology: Processes, Models, and Applications. Oxford University Press, Oxford.

[42] MacArthur, R., Levins, R., 1967. The limiting similarity, convergence, and divergence of coexisting species. The American Naturalist 101, 377–385.

[43] Munday, P.L., 2004. Competitive coexistence of coral-dwelling fishes: The lottery hypothesis revisited. Ecological Society of America 85, 623–628.

[44] Nagelkerke, L.A.J., Rossberg, A.G., 2014. Trophic niche-space imaging, using resource and consumer traits. Theoretical Ecology 7, 423–434.

[45] Pascual, M., Dunne, J.A., 2005. From small to large ecological networks in a dynamic world, in: Pascual, M., Dunne, J.A. (Eds.), Ecological Networks: Linking Structure to Dynamics in Food Webs (Santa Fe Institute Studies on the Sciences of Complexity). Oxford University Press, pp. 3–24.

[46] Persson, L., Diehl, S., Johansson, L., Andersson, G., Hamrin, S.F., 1992. Trophic interactions in temperate lake ecosystems: A test of food chain theory. The American Naturalist 140, 59–84.

[47] Petchey, O., Beckerman, A., Riede, J., Warren, P., 2008. Size, foraging, and food web structure. Proceedings of the National Academy of Sciences of the United States of America 105, 4191–4196.

[48] Peters, R.H., 1986. The Ecological Implications of Body Size (Cambridge Studies in Ecology). 1 ed., Cambridge University Press.

[49] Polis, G.A., 1991. Complex trophic interactions in deserts: An empirical critique of food-web theory. The American Naturalist 138, 123–155.

[50] Ricklefs, R.E., Bermingham, E., 2002. The concept of the taxon cycle in biogeography. Global Ecology and Biogeography 11, 353–361.

[51] Riede, J.O., Brose, U., Ebenman, B., Jacob, U., Thompson, R., Townsend, C.R., Jonsson, T., 2011. Stepping in eltons footprints: a general scaling model for body masses and trophic levels across ecosystems. Ecology Letters 14, 169–178.

[52] Rohr, R.P., Scherer, H., Kehrli, P., Mazza, C., Bersier, L., 2010. Modeling food webs: Exploring unexplained structure using latent traits. The American Naturalist 176, 170–177.

[53] Rosenzweig, M.L., Brown, J.S., Vincent, T.L., 1987. Red queens and ess: the coevolution of evolutionary rates. Evolutionary Ecology 1, 59–94.

[54] Rossberg, A., Matsuda, H., Amemiya, T., Itoh, K., 2006. Food webs: Experts consuming families of experts. Journal of Theoretical Biology 241, 552 – 563.

[55] Rossberg, A.G., Brännström, Å., Dieckmann, U., 2010. Food-web structure in low-and high-dimensional trophic niche spaces. Journal of The Royal Society Interface 7, 1735–1743.

[56] Rossberg, A.G., Ishii, R., Amemiya, T., Itoh, K., 2008. The top-down mechanism for body-mass-abundance scaling. Ecology 89, 567–580.

[57] Roughgarden, J., Pacala, S., 1989. Taxon cycle among Anolis lizard populations: review of evidence.

[58] Saetre, P., Bååth, E., 2000. Spatial variation and patterns of soil microbial community structure in a mixed sprucebirch stand. Soil Biology and Biochemistry 32, 909 – 917.

[59] Scheffer, M., van Nes, E.H., 2006. Self-organized similarity, the evolutionary emergence of groups of similar species. Proceedings of the National Academy of Sciences 103, 6230–6235.

[60] Stouffer, D.B., Camacho, J., Amaral, L.A.N., 2006. A robust measure of food web intervality. Proceedings of the National Academy of Sciences 103, 19015–19020.

[61] Stouffer, D.B., Camacho, J., Jiang, W., Nunes Amaral, L.A., 2007. Evidence for the existence of a robust pattern of prey selection in food webs. Proceedings of the Royal Society of London B: Biological Sciences 274, 1931–1940.

[62] Stouffer, D.B., Rezende, E.L., Amaral, L.A.N., 2011. The role of body mass in diet contiguity and food-web structure. Journal of Animal Ecology 80, 632–639.

[63] Strong, D.R., 1992. Are trophic cascades all wet? differentiation and donor-control in speciose ecosystems. Ecology 73, 747–754.

[64] Sutherland, J., of Environmental Conservation, N.Y.S.D., 1989. Field surveys of the biota and selected water chemistry parameters in 50 adirondack mountain lakes .

[65] Takahashi, D., Brännström, Å., Mazzucco, R., Yamauchi, A., Dieckmann, U., 2011. Cyclic transitions in simulated food-web evolution. Journal of Plant Interactions 6, 181–182.

[66] Takahashi, D., Brännström, Å., Mazzucco, R., Yamauchi, A., Dieckmann, U., 2013. Abrupt community transitions and cyclic evolutionary dynamics in complex food webs. Journal of Theoretical Biology 337, 181 – 189.

[67] Tokita, K., Yasutomi, A., 2003. Emergence of a complex and stable network in a model ecosystem with extinction and mutation. Theoretical population biology 63, 131–146.

[68] Turchin, P., 2003. Complex population dynamics: a theoretical/empirical synthesis. volume 35. Princeton University Press.

[69] Vucic-Pestic, O., Rall, B.C., Kalinkat, G., Brose, U., 2010. Allometric functional response model: body masses constrain interaction strengths. Journal of Animal Ecology 79, 249–256.

[70] Williams, R.J., Martinez, N.D., 2000. Simple rules yield complex food webs. Nature 404, 180–183.

[71] Williams, R.J., Martinez, N.D., 2004. Limits to trophic levels and omnivory in complex food webs: Theory and data. The American Naturalist 163, 458–468.

[72] Williams, R.J., Martinez, N.D., 2008. Success and its limits among structural models of complex food webs. Journal of Animal Ecology 77, 512–519.

[73] Wilson, E.O., 1961. The nature of the taxon cycle in the melanesian ant fauna. The American Naturalist 95, 169–193.

[74] Yodzis, P., Innes, S., 1992. Body size and consumer-resource dynamics. The American Naturalist 139, 1151–1175.

[75] Zhang, L., Hartvig, M., Knudsen, K., Andersen, K., 2014. Size-based predictions of food web patterns. Theoretical Ecology 7, 23–33.

Appendix A. Appendix

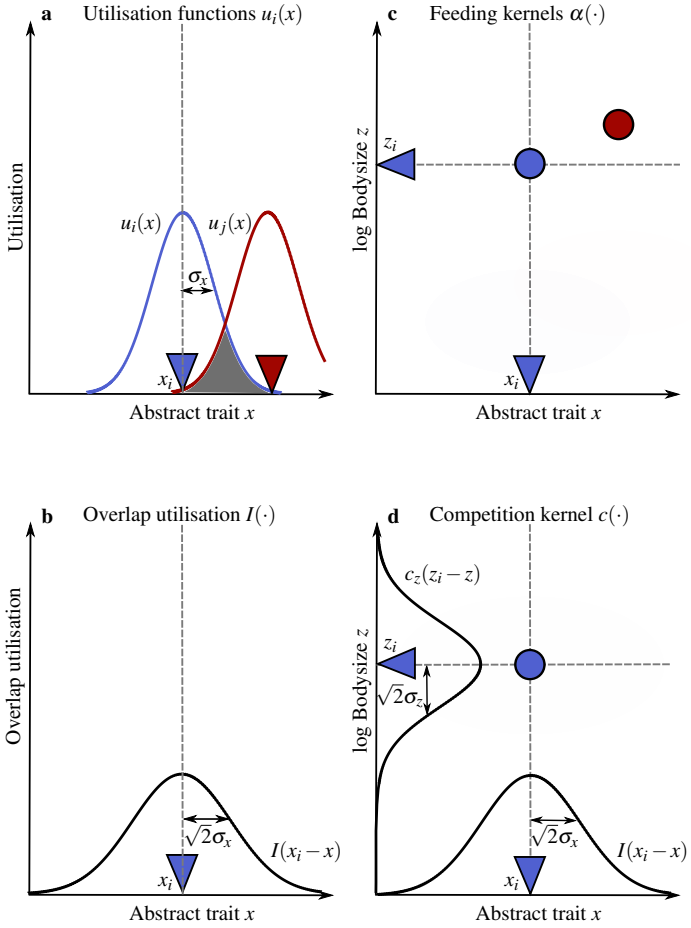

Figure A.8: Derivation of the interaction kernels. **Left Column:** Deduction of the utilisation overlap $I(\cdot)$, describing the interaction strength along the abstract trait dimension. **a:** Utilisation function $u_k(x)$, which can be interpreted as the distribution of morph k along the abstract trait axis. Following MacArthur and Levins [42], we assume that a morph k utilises a certain range around its abstract trait value x_k

$$u_k(x) = \frac{1}{\sigma_x \sqrt{2\pi}} \exp\Big(- \frac{(|x_i - x|)^2}{2\sigma_x^2} \Big),$$

which has a width of σ_x. **b:** The utilisation overlap $I(\cdot)$ between two morphs is given by the normalized overlap [59] of their utilisation functions:

$$I(x_i, x_j) = \frac{\int_{-\infty}^{\infty} dx u_i(x) u_j(x)}{\int_{-\infty}^{\infty} dx \; u_i^2(x)} = \frac{1}{\sigma_x \sqrt{4\pi}} \exp\Big(- \frac{(|x_i - x_j|)^2}{4\sigma_x^2} \Big),$$

resulting in a Gaussian function with a width of $\sqrt{2}\sigma_x$. **Right Column:** Derivation of the competition kernel $c(\cdot)$ in two dimensional trait space. **c:** Feeding kernels $\alpha(\cdot)$ of two morphs in two dimensional trait space. **d:** Competition kernel $c(\cdot)$, given by the normalised overlap of the bodysize feeding kernel $c_z(\cdot) \sim \int_{-\infty}^{\infty} dx \; \alpha(z_i - z)\alpha(z_j - z)$, multiplied with the overlap $I(\cdot)$ of their utilisation functions. This results in a two dimensional Gaussian. The competition ranges are proportional to the width of the kernels of a single morph and are therefore no independent parameters.

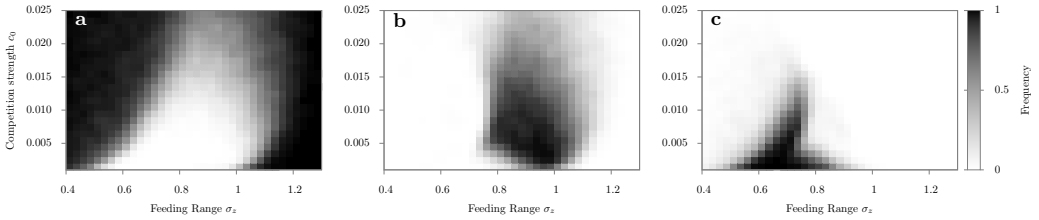

Figure A.9: Frequencies of occurrence (indicated in grey shading) of the different community types in repeated simulations, in dependency of the feeding range, σ_z, and competition strength, c_0 (compare to Fig. 2). **a:** Communities with no trophic structure, **b:** evolutionary static food webs, and **c:** evolutionary dynamic food webs. See Section 2.3 for more details.

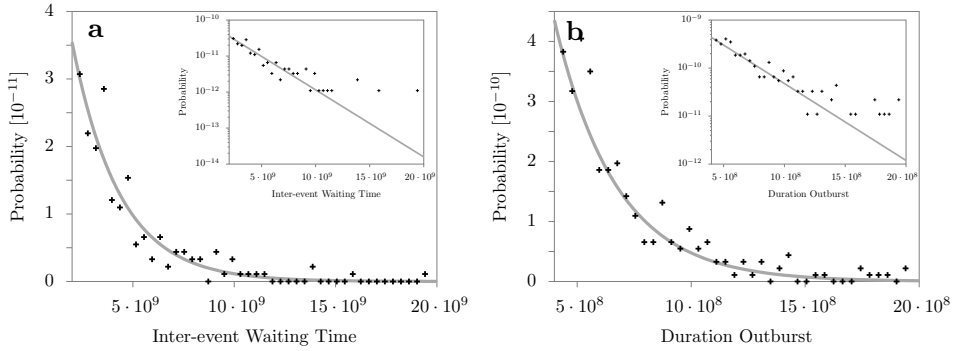

Figure A.10: Inter-event waiting time and duration of evolutionary outbursts. **a:** Probability density function of the inter-event waiting times between outbursts. **b:** Probability density function of the outburst duration. The insets in **a** and **b** show the same data in a semi-logarithmic plot. Solid lines show exponential functions fitted to the data, which yields typical time constants of $2.3 \pm 0.2 \cdot 10^9$ (inter-event waiting time) and $2.7 \pm 0.1 \cdot 10^8$ (outburst duration). Note, the different time scales between inter-event waiting times, the duration of single outbursts, the downward evolutionary motion and the breakdown of an evolutionary outburst (see also Fig. 5). The same parameters as in Fig. 5 were used. In total 2300 events were recorded.

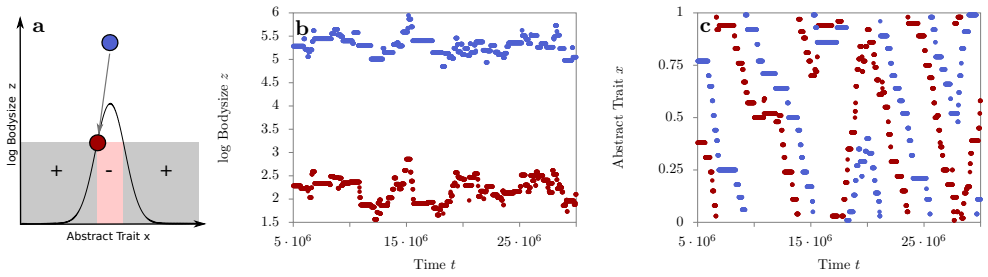

Figure A.11: Predator-prey arms race. The system was parametrised (by setting $I = 100, \sigma_x = 0.17, \sigma_z = 0.7, c_0 = 0.001$) so that it only contains a single predator (blue) and prey (red) morph. **a:** Positioning of predator and prey morphs (circles) in two-dimensional niche space and sketch of the feeding strength (solid line) and the prey's fitness landscape in dependence of the value of the abstract trait. Coloured shading indicates regions of negative (red) and positive (grey) fitness. **b,c:** Evolution of bodysize and abstract trait of the predator and prey morph, demonstrating the emergence of bodysize oscillations (**b**) and arms races (**c**). The predator is chasing the prey along the abstract trait axis. It is even possible for this movement to change directions: If the predator's and prey's abstract traits are similar, the mutational range can exceed the area of negative fitness (red area in **a**) and a mutant can occur on the other side of the predator.

Appendix A.1. Red-queen dynamics in a small community

In a small community, which can contain only two morphs, one predator and one prey, it is possible to disentangle population dynamics and evolutionary processes (Fig A.11). Assume that the predator in this system has bodysize z_1 and abstract trait value x_1. The prey's fitness increases the further it is separated from the centre $(z_1 - d, x_1)$ of the predator's feeding range (see sketch in Fig. A.11a). As such, over evolutionary time, the prey will evolve away from this centre due to a sequence of invasions by more fit mutants. This, in turn, decreases the predator's fitness, and consequently, the predator follows the prey by the same evolutionary process, Fig. A.11b,c. The result is an evolutionary arms race or red-queen dynamics [1, 53, 21] between predator and prey.

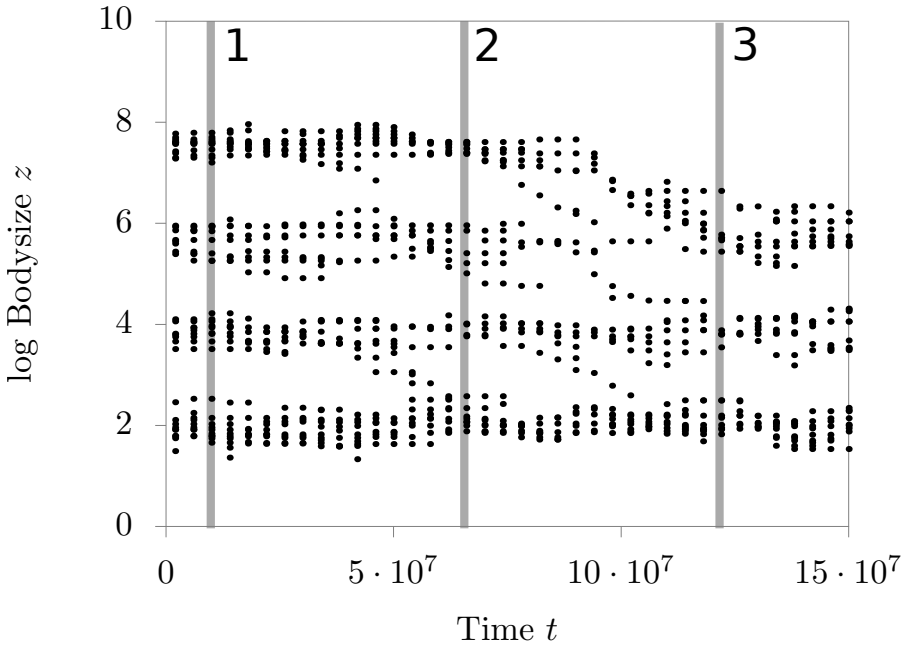

Figure A.12: Snapshot of the termination of an evolutionary outburst for the system shown in Fig. 5 (note that the time scale has been reduced to allow the dynamics of this process to be seen clearly). Evolutionary outbursts are characterised by the presence of an additional, unstable, layer of morphs at high bodysizes (**1**). The onset of termination occurs when there is insufficient resource flow to this layer, due to decreased morph density in the bodysize layer below it (**2**). The morphs in the upper bodysize layer slowly decrease their bodysize via numerous mutational steps, leaving this layer empty (**3**).

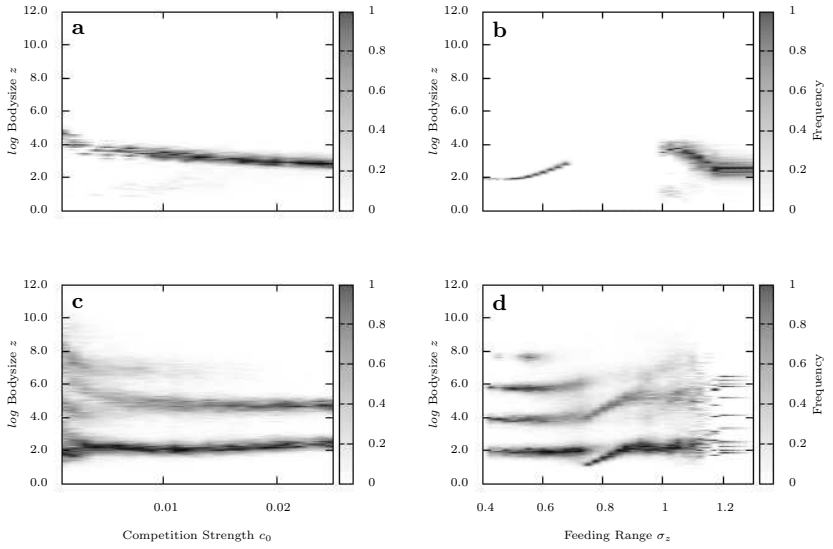

Figure A.13: Bodysize spectrum of communities with and without a trophic structure, along the cross sections of the parameter space, shown in Fig. 2. The first column shows cross section I (different values of competition strength c_0, fixed $\sigma_z = 1$). The second column depicts cross section II (different values of feeding range σ_z, fixed $c_0 = 0.005$). For each parameter we averaged over 100 simulation runs. **a,b:** Bodysize probability density function of communities without a trophic structure. **c,d:** Bodysize probability density function of communities with a trophic structure.